# INTERNATIONAL SOCIETY FOR SOIL MECHANICS AND GEOTECHNICAL ENGINEERING



This paper was downloaded from the Online Library of the International Society for Soil Mechanics and Geotechnical Engineering (ISSMGE). The library is available here:

https://www.issmge.org/publications/online-library

This is an open-access database that archives thousands of papers published under the Auspices of the ISSMGE and maintained by the Innovation and Development Committee of ISSMGE.

# Analysis of the impact of climate change on the landslides along the mountain highway in central Taiwan

Analyse de l'impact du changement climatique sur les glissements de terrain le long de l'autoroute de montagne au centre de Taiwan

Keh-Jian Shou, Zora Lin

Department of Civil Engineering, National Chung-Hsing University, Taiwan, kishou@dragon.nchu.edu.tw

ABSTRACT: Climate change caused by global warming affects Taiwan significantly for the past decade. The increasing frequency of extreme rainfall events, in which concentrated and intensive rainfalls generally cause geohazards including landslides. Considering the existence of various types of landslides and the protection targets, this study aims to analyse the landslide susceptibility along the Nantou County Road # 89 in Central Taiwan. This study employs rainfall frequency analysis and the atmospheric general circulation model (AGCM) downscaling estimation to obtain the temporal rainfall distributions, then the landslide susceptibility was estimated for the study area. Based on the Li-DAR and the borehole data, the temporal behavior and the complex mechanism of large scale deep-seated landslides were also analyzed.

RÉSUMÉ: Les changements climatiques causés par le réchauffement climatique affectent considérablement Taiwan ces dix dernières années. La fréquence croissante des pluies extrêmes, où les pluies concentrées et intenses provoquent généralement des risques géologiques, y compris des glissements de terrain. Compte tenu de l'existence de différents types de glissements de terrain et des objectifs de protection, cette étude vise à analyser la sensibilité aux glissements de terrain le long de la route 89 du comté de Nantou dans le centre de Taiwan. Cette étude utilise l'analyse de la fréquence des précipitations et l'estimation de la réduction de la distribution du modèle de circulation générale atmosphérique (AGCM) pour obtenir les distributions temporelles des précipitations, puis la susceptibilité aux glissements de terrain a été estimée pour la zone d'étude. En se fondant sur les données du DAR et des sondages, le comportement temporel et le mécanisme complexe des glissements de terrain à grande profondeur ont également été analysés.

KEYWORDS: landslide hazard, climate change, mountain highway, landslide susceptibility

#### 1 INTRODUCTION

The climate change affects Taiwan significantly by an increasing frequency of extreme rainfall events, in which induced large scale landslides. Considering the existence of various types of large scale landslides and the protection targets, this study aims to analyze the landslide susceptibility along the Nantou County Road # 89 of Taiwan (see Fig.1). For the predictive analysis of landslide susceptibility, this study employed AGCM downscaling estimation. For the adopted large scale landslides (see Fig. 2), based on the information from boreholes, the temporal behavior and the complex mechanism of large scale landslides were analyzed in local scale. Based on the results, the pros and cons of the analysis in both scale were discussed, which could be applied for the risk assessment and management.

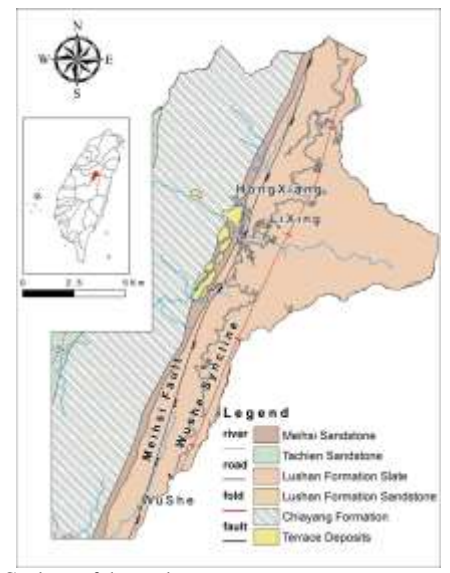


Figure 1. Geology of the study area



Figure 2. Large landslide along the Nantou County Road # 89

# 2 METHODOLOGIES

Landslide inventories, SPOT satellite images, borehole data were collected in the study area, including 5 major deep-seated landslides along the County Road #89. In addition, mobile laser ranging was performed along the road to obtain the 0.1 LiDAR data. The obtain information and data were used for the shallow and deep-seated landslides in different scale.

## 2.1 Landslides interpretation

This study adopts the NDVI-slope angel criterion, in which the normalized differential vegetation index (NDVI) is from satellite images and the slope angle is from digital elevation model (DEM). And improving the accuracy of landslide identification in shadow areas with different screening indexes,

including brightness (BRI, Hsieh et al 2011), greenness (GI, Liu et al 2012; Lin et al 2013), and vegetation mask (Beumier and Idrissa 2014). The compare of landslides interpretation in different indexes as Table 1. A1 is the number of landslide cells interpreted as landslide, A3 is the number of landslide cells not interpreted as landslide, A2 is the number of non-landslide cells interpreted as non-landslide, A4 is the number of non-landslide cells interpreted as landslide.

Table 1. Comparison of the Criteria for Automatic Landslide Interpretation.

Criterion	Accuracy of Landslide Cells A1/ (A1+A3)	Accuracy of Non-landslid Cells A4/ (A2+A4)	Accuracy of Total Cells (A1+A4)/ (A1+A2+ A3+A4)
Slope=20%, NDVI=0, BRI=40	6.6	0 99.6	53 98.49
Slope=20%, NDVI=0, GI=0.25	7.1	1 99.6	52 98.49
Slope=20%, NDVI=0.2	21.0	2 97.7	79 96.86
Slope=20%, NDVI=0.2, BRI=40	18.8	1 97.8	96.90
Slope=20%, NDVI=0.2, GI=0.25	20.4	0 97.9	97.00
Slope=20%, NDVI=0.2, BRI=60	7.0	4 98.4	16 97.34

#### 2.2 Landslide-rainfall index (Id)

For a specific typhoon event, by the overlapping function of GIS, the accumulated rainfall and rainfall intensity data at the landslide locations can be extracted and plotted in graph of accumulated rainfall and rainfall intensity (see Fig. 3). The landslide-rainfall index (Id) is defined by the distances d1 and d2 from the unknown point to the linear thresholds as d2/(d1+d2) (Shou et al, 2015).

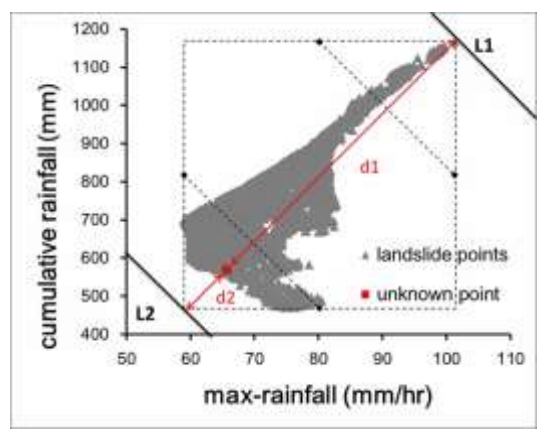


Figure 3. The landslide-rainfall index (Id) is defined as d2/(d1+d2).

It ranges between 0 and 1. As Id approaches 1, the slope becomes increasingly susceptible to rainfall-induced landslide. On the contrary, as the point of the rainfall of potential landslide approaches the lower threshold, or as Id approaches 0, the slope becomes less susceptible to landslide.

# 2.3 Landslide susceptibility models

This study adopts the In Logistic Regression Method for the landslide susceptibility analysis. Its performance was compared for the analyses of 2004 Mindulle, 2009 Morakot, and 2012 Saola. Based on the training samples, which comprised a group of data points or data locations, categorized as landslide and non-landslide. The data layer of each factor was then placed upon the landslide and non-landslide layers, and the correlation between each factor and landslides was used to conduct binary

logistic regression. For the susceptibility model obtained by logistic regression, this study employed the receiver operating characteristic (ROC) curve (Swets 1988), in which the area under the curve (AUC) of the ROC curve was used to evaluate the prediction accuracy. Generally, the larger the AUC values the better. As the area approaches 0.5, the result may not necessarily be superior to that of a random selection. AUC values of less than 0.5 are not worth employing.

#### 3 LANDSLIDE SUSCEPTIBILITY ANALYSIS

This study adopts the Logistic Regression Method for the landslide susceptibility analysis. The model based on 2004 Mindulle can be expressed as

P=0.663F1+0.055F2-0.317F3-0.062F4-0.301F5-0.216F6-0.093F7+0.081F8-2.451F9+0.295 (1)

where P is the logistic function, F1 is the slope angle, F2 is the elevation, F3 is the aspect, F4 is the distance to fault, F5 is the distance to river, F6 is the distance to road, F7 is the dip slope index (Ids), F8 is the landslide-rainfall index (Id), and F9 is the normalized differential vegetation index (NDVI). Eq. (1) can be used to calculate the landslide susceptibility based on the predicted rainfalls, including various extreme weather scenarios as below.

By using Eq. (1), we can estimate the landslide susceptibility of 2009 Morakot and 2012 Saola based on their specific rainfalls. The ROC curves for these estimations shows the AUC values are 0.806 for 2009 Morakot and 0.717 for 2012 Saola, which also reveal an acceptable performance of the 2004 Mindulle model.

For the predictive analysis, the rainfall in the future was estimated by the climate change model introduced as below. The Taiwan Climate Change Projection and Information Platform Project (TCCIP), analyzes the results from the assessment reports of the United Nations Intergovernmental Panel on Climate Change (IPCC), results of 2004Mindulle and Top1 Typhoon show as Figs. 4~5, and compare of cells number as Table 2.

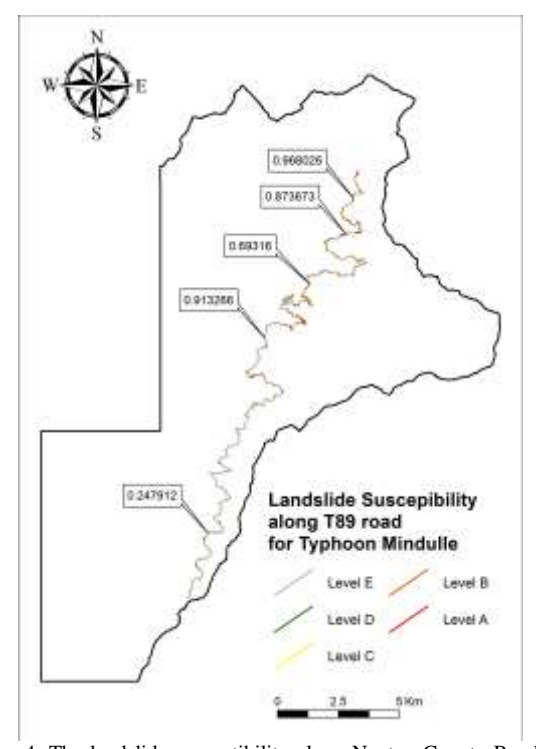


Figure 4. The landslide susceptibility along Nantou County Road #89 estimated by 2004 Mindulle model

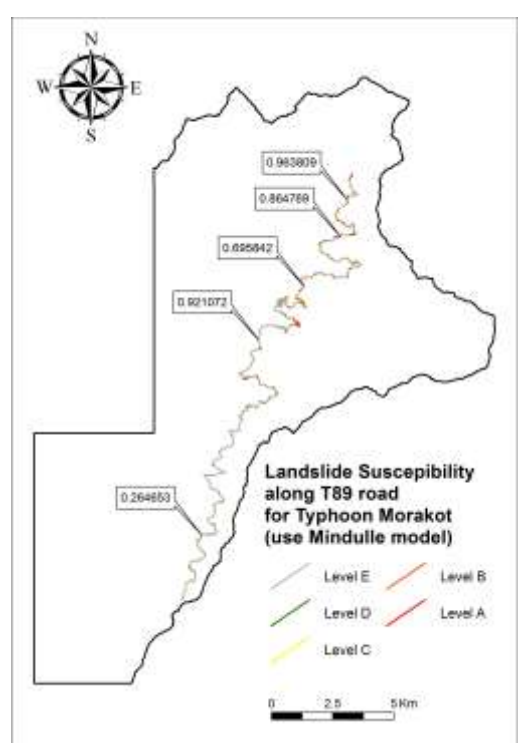


Figure 5. The landslide susceptibility along Nantou County Road #89 estimated by the TCCIP Top1 Typhoon

Table 2 Comparison of the Landslide Susceptibility and Risk Ranking of the Large Scale Landslides

Site	Mindulle Landslide Su	sceptibility	Predict Top1 Typhoon(2075-2099) Landslide Susceptibility		
	Value	Ranking	Value	Ranking	
12k+300	0.968026	1	0.966557	1	
15k+850	0.873673	3	0.8683	3	
22k+530	0.69316	4	0.688009	4	
32k+500	0.913266	2	0.914724	2	
49k+000	0.247912	5	0.271284	5	

### 4 ANALYSIS OF MAJOR LARGE SCALE LANDSLIDES

For the adopted large scale landslides (see Fig. 2), based on the information from boreholes, the temporal behavior a nd the complex mechanism of large scale landslides were analyzed in local scale. Fig. 6 shows locations of the 5 st udied major profile. In this study, the limit equilibrium an alyses software Slide 6.0 (Rocscience 2015) was applied.

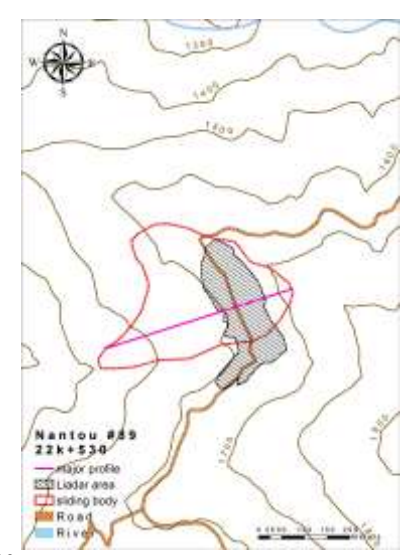
In the analyses, three types of geo-material were assumed, i.e., highly weathered slate in the boundary layer, medium weathered slate in the middle layer, and fresh slate in the bottom. Their material properties were determined based on the report of exploration (Xie-Sheng Engineering Consulting, 2014). For a better comparison, this study considered three different groundwater conditions, i.e., dry (no groundwater), 1/2 ground water level, and full ground water level. The results of equilibrium analyses were summarized in Table 3.



(a) 12k+300

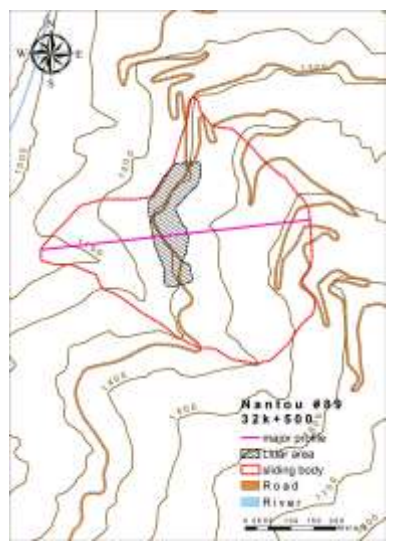


(b) 15k+850

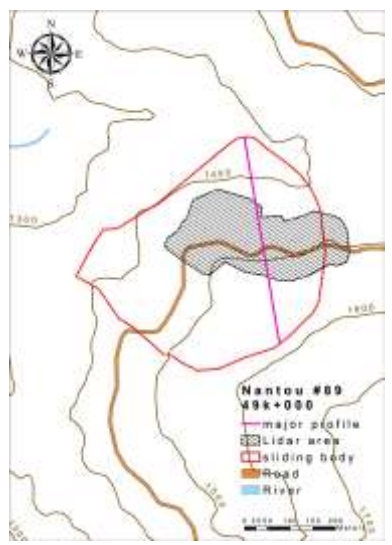


(c) 22k+530

Figure 6. The profiles of the large scale landslides. (continued)



(d) 32k+500



(e) 49k+000

Figure 6. The profiles of the large scale landslides

Table 3 Comparison of the Safety Factors and Risk Ranking of the

Site	No Groundwater		1/2 Groundwater		Full Groundwater	
	FS,min	Rank	FS,min	Rank	FS,mi	Rank
12k+300	0.700 (toe)	2	0.594 (toe)	2	0.456 (toe)	2
15k+850	0.659 (whole)	1	0.539 (head)	1	0.384 (head)	1
22k+530	1.058 (head)	4	0.841 (head)	4	0.577 (head)	3
32k+500	1.082 (middle)	5	0.877 (middle)	5	0.61 (middle)	5
49k+000	0.978 (whole)	3	0.796 (whole)	3	0.603 (whole)	4

# 5 CONCLUSION

In this study, rainfall frequency analysis and the atmospheric general circulation model (AGCM) downscaling estimation were applied to understand the temporal rainfall trends and distributions in the study area. The susceptibility analysis in catchment scale and local scale were performed for the hazard assessment of the mountain highway, i.e., Nantou County Road #89 in Central Taiwan. The hazard of the major landslides can be ranked to prioritize the hazard mitigation. It is worth noting that the results of local scale analysis also suggest a similar hazard ranking of these landslides, i.e. the sites 15k+850 and 12k+300 are the most dangerous.

#### 6 ACKNOWLEDGEMENTS

This research was made possible by the financial support of the National Science Council (Project No. 102-2625-M-005-001-MY2) of Taiwan. We also deeply appreciate the databases and support from the research groups conducting the Central Geological Survey project (Project No. 97-5826901000-05).

#### 7 REFERENCES

Beumier, C. and Idrissa, M. (2014). Building detection with multi-view colour infrared imagery. EARSeL eProceedings 13:77-84.

Hsieh, Y.T., Wu, S.T., Liao, C.S., Yui, Y.G., Chen, J.C., and Chung, Y.L. (2011). Automatic extraction of shadow and non-shadow landslide area from ADS40 image by stratified classification. Geoscience and remote sensing, IEEE International symposium – IGARSS: 3050-3053.

Lin, E.J., Liu, C.C., Chang, C.H., Cheng, I.F., and Ko, M.H. (2013). Using the FORMOSAT-2 high spatial and temporal resolution multispectral image for analysis and interpretation of landslide disasters in Taiwan. Journal of Photogrammetry and Remote Sensing 17(1):31-51.

Liu, J.K., Hsiao, K.H., and Shih, T.Y. (2012). A geomorphological model for landslide detection using airborne LIDAR data. Journal of Marine Science and Technology 20(6):629-638.

Rocscience Inc. (2015). User manual of Slide 6.0 – 2D limit equilibrium analysis of slope stability.

Shou, K.J. and Yang, C.M. (2015). Predictive analysis of landslide susceptibility under climate change conditions – a Study on the Chingshui River Watershed of Taiwan. Engineering Geology 192:46-62.

Swets, J.A., 1988. Measuring the accuracy of diagnostic systems. Science 240: 1285-1293.

Xie-Sheng Engineering Consulting (2014). Minitoring of Major Landslides along the Nantou County Road #89 after 2012 Typhoon Talim. Report to the Nantou County Government